Supplementary Information

# Tunability of Hybridized Plasmonic Waveguide Mediated by Surface Plasmon Polaritons

Ming-Ming Jiang[1], Hong-Yu Chen[1,2], Chong-Xin Shan[1,*], and De-Zhen Shen[1,*]

[1] *State key Laboratory of Luminescence and Applications, Changchun Institute of Optics, Fine Mechanics and Physics, Chinese Academy of Sciences, Dongnanhu Road 3888, Changchun, 130033, People's Republic of China*

[2] *Graduate University of the Chinese Academy of Sciences, Beijing, 100049, People's Republic of China*

## 1 Coupled mode theory

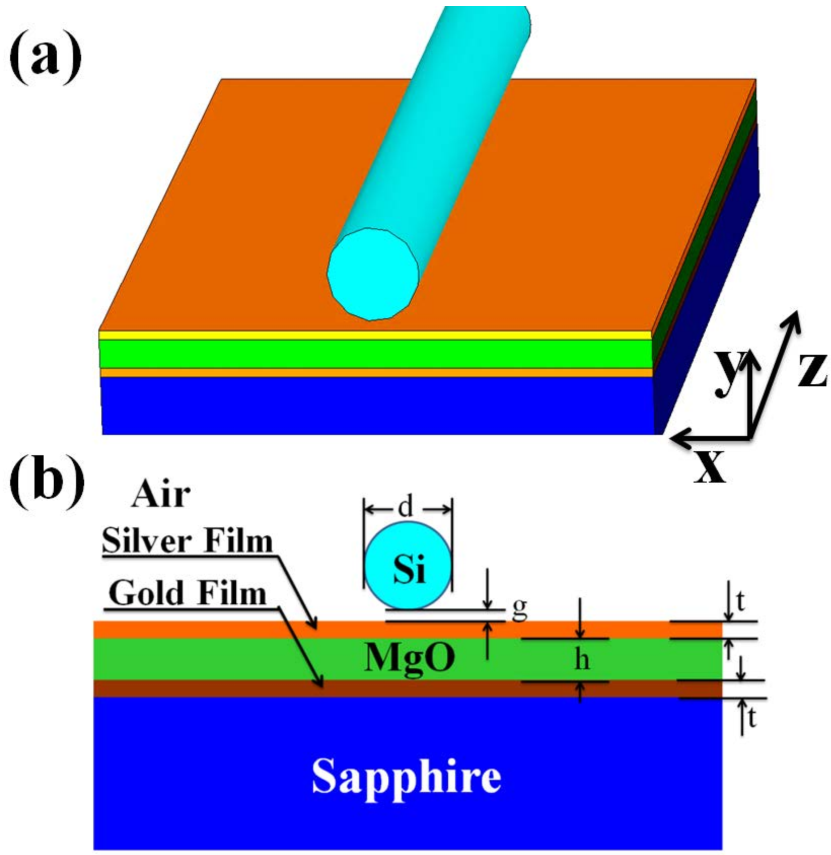


Figure S1: The tunable hybridized plasmonic waveguide: A dielectric cylindrical nanowire of permittivity $\varepsilon_c$ and diameter d is separated from the upper metallic half-space of permittivity $\varepsilon_{m1}$ by a nanoscale dielectric gap of permittivity $g$ and width $t$. The upper medium is a dielectric of permittivity $\varepsilon_{d1}$. The lower metallic half-space of permittivity $\varepsilon_{m2}$, the intermediate low index material permittivity $h$. $\varepsilon_c = 12.25$ (Si) and $\varepsilon_{d1} = 2.25$ ($SiO_2$), $\varepsilon_{d2} = 2$, $\varepsilon_{substrate} = 1.56$, at the telecommunications wavelength $\lambda_0 = 1.55\mu m$. The upper metallic region is silver with a permittivity of $\varepsilon_{m1} = -129 + 3.3i$, and the low metallic region is gold with a permittivity of $\varepsilon_{m1} = -110 + 10i$. The centre of the cylinder defines the origin (x=y=0).

Here, we propose a novel hybrid plasmonic waveguide shown in Fig.S1 consisting of a high-permittivity semiconductor nanowire (cylinder waveguide) embedded in a low-permittivity dielectric near upper metal surface (D-SPP waveguide) and there is the other metal film, separated from the upper metal film with a distance $h$. To solve the problem, here we propose an alternative method by tuning the thickness of dielectric cladding on the low metal film to change the effective mode index. From the geometry, we can see that the model is composed of the cylinder-like and DSPP-like modes. In this section, we will use the coupled mode theory to describe the mode hybridization of three modes using a two dimensional matrix representation. The hybrid mode reads

$$|\psi_{\pm}(d,g,h)\rangle = a_{\pm}(d,g,h)|\psi_{cyl}(d)\rangle + b_{\pm}(d,g,h)|\psi_{dspp}(h)\rangle \tag{1}$$

where $a_{\pm}(d,g,h)$ and $b_{\pm}(d,g,h)$ are the amplitudes of the constituent cylinder mode $|\psi_{cyl}(d)\rangle = \{1 \quad 0\}^T$ and D-SPP $|\psi_{dspp}(h)\rangle = \{0 \quad 1\}^T$ basis modes, respectively. The normalized condition is $|a_{\pm}(d,g,h)|^2 + |b_{\pm}(d,g,h)|^2 = 1$. All modes may be characterized in terms of an effective index, which is proportional to the real part of its eigenvalue quantifying the phase velocity in the direction of propagation. The magnitude of the in-plane surface plasmon wavevector, $k_{dspp} = n_{dspp}k_0$ corresponds to an effective index $n_{dspp}$, where $k_0$ is the free-space wavenumber. The effective index of the fundamental cylinder mode, $n_{cyl}(d)$, the modes of the coupled system are characterized by the system of equations

$$\begin{pmatrix} n_{cyl}(d) & \kappa(d,g,h) \\ \kappa(d,g,h) & n_{dspp}(h_2) \end{pmatrix} \begin{pmatrix} a_{\pm}(d,g,h) \\ b_{\pm}(d,g,h) \end{pmatrix} = n_{\pm}(d,g,h) \begin{pmatrix} a_{\pm}(d,g,h) \\ b_{\pm}(d,g,h) \end{pmatrix}, \tag{2}$$

where $\kappa(d,g,h)$ is the coupling strength between cylinder mode and DSPP modes, which can be derived as

$$\kappa(d,g,h) = \sqrt{(n_{\pm}(d,g,h) - n_{dspp}(h))(n_{\pm}(d,g,h) - n_{cyl}(d))} \tag{3}$$

From the matrix of the hybrid mode, we can calculate the results

$$|a_{\pm}(d,g,h)|^2 = \frac{\kappa(d,g,h)^2}{(n_{\pm}(d,g,h) - n_{cyl}(d))^2 + \kappa(d,g,h)^2} \tag{4}$$

For the sake of describing the mode characteristics of the hybrid mode, we need a mode character, $|a_{+}(d,g,h)|^2$ to represent the superposition of the cylinder waveguide mode and the DSPP mode based on the coupled-mode theory, $n_{hyb}(d,g,h) = n_{+}(d,g,h)$

$$|a_{+}(d,g,h)|^2 = \frac{n_{hyb}(d,g,h) - n_{dspp}(h)}{(n_{hyb}(d,g,h) - n_{dspp}(h)) + (n_{hyb}(d,g,h) - n_{cyl}(d))} \tag{5}$$

From this equation, $|a_{+}(d,g,h)|^2 = 0.5$ is the breakthrough point of the hybrid mode. At the critical coupling diameter $d_c$, the hybrid mode has equal DSPP and cylinder characteristics, corresponding to the condition $n_{cyl}(d) = n_{dspp}(h)$. When $|a_{+}(d,g,h)|^2 > 0.5$ the mode is cylinder-like and DSPP-like otherwise. The value $|a_{+}(d,g,h)|^2$ is a measure to determine a large portion of light energy is located in the cylinder nanowire or tended to be confined in the gap region between the dielectric nanowire and metal films(*X. Zhang, Nature Photonics, 2008, 2, 496C500*).

Upon this model, we find out that the thickness $h$ of low index layer gap can be used to adjust the mode characteristics, compared with model.

From the pictures S3 and S4, it can be found that the thickness of the metal film has great effect effect on the electromagnetic energy distribution. When the thickness of the metal film changes in the range of 20 nm, part of electromagnetic filed energy can be distributed in the dielectric spacer region; When the thickness of the metal film exceeds over 20 nm, there is little electromagnetic energy distributed in the dielectric spacer between double metal films.

Figure S5 and S6 demonstrate that the spacer thickness has great effect on the tunability of mode characteristics for the hybridized plasmonic waveguides: the mode effective index, coupling strength, the mode character, as well as the hybrid mode's propagation distance.

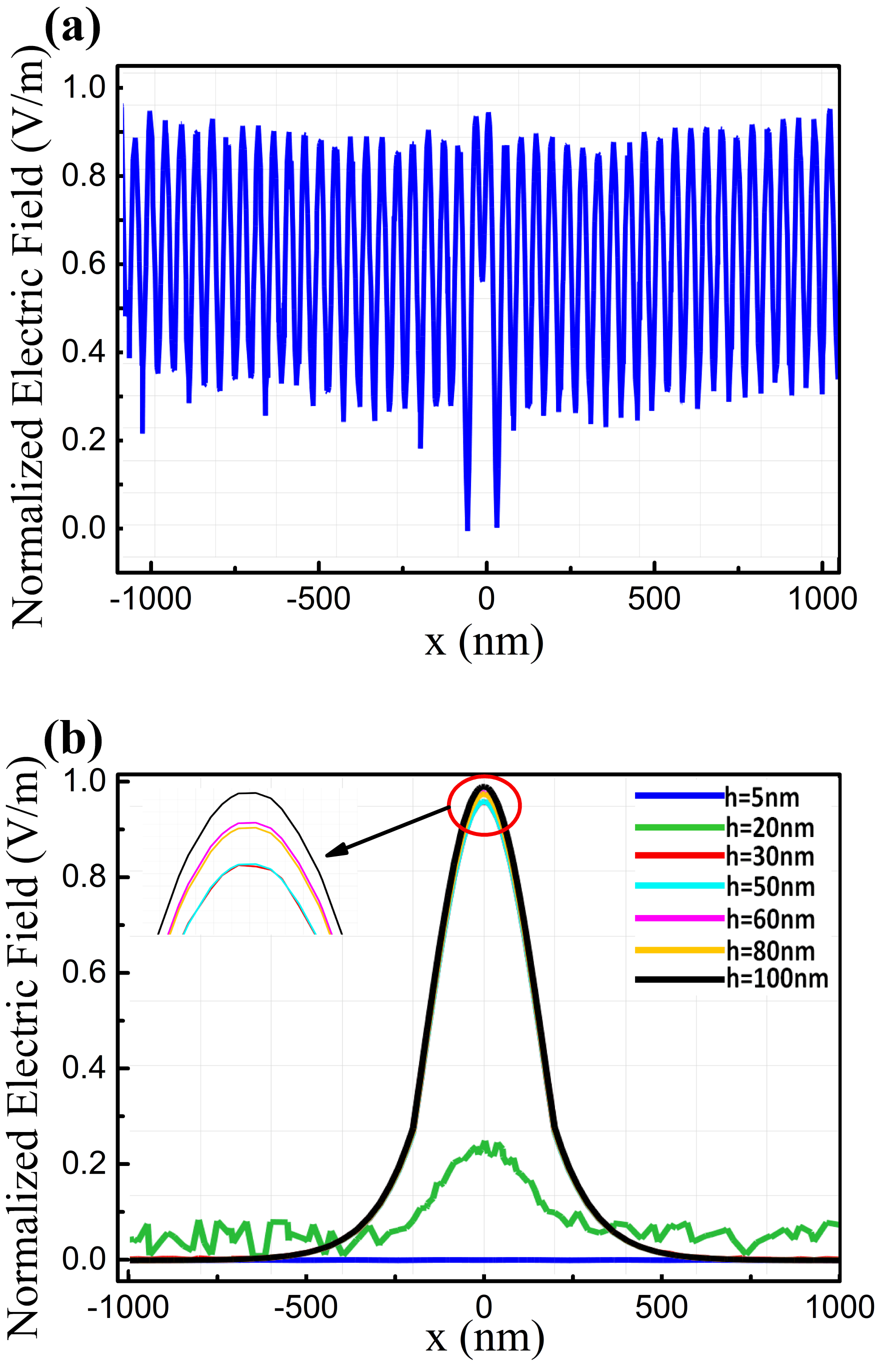


Figure S2: (a) Confinement of electromagnetic field *E(x,y)* distribution in the low-index dielectric gap spacer region with $d = 500$ nm and $g = h = 5$ nm along y = 0 when the thickness of metal films $t = 20$ nm, which is consistent with the experimental results; (b) The transfer process of confinement of electric field E(x,y) distribution in the dielectric gap spacer region with $d = 500$ nm and $g = 5$ nm along y = 0 with the variable spacer thickness $h$ shown in the inset, where the electrical field distribution of the gap spacer distance $h = 5$ nm corresponding to the result above (a). $*$ The corresponding electromagnetic field energy distribution can be referred to the additional information materials.

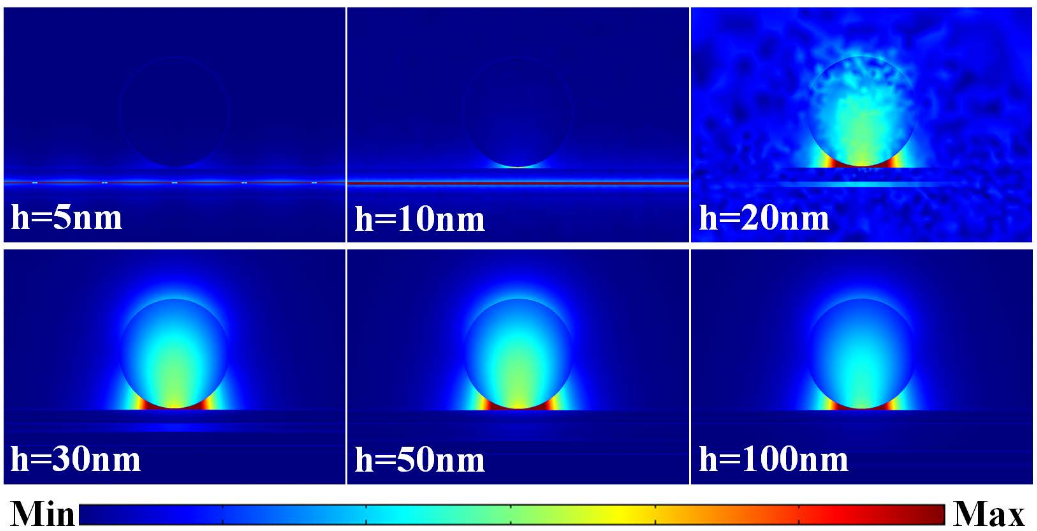


Figure S3: Electromagnetic energy density distributions with the variable spacer thickness h with the thickness of metal films t = 50nm. When the spacer distance h = 5 nm, electromagnetic energy is mainly distributed in the spacer; Increasing the spacer distance, the transfer process of electromagnetic energy will transit from the dielectric spacer gap region to the gap area between cylinder and the upper metal film. The critical value of dielectric layer thickness is h = 20 nm. As the spacer thickness h exceeded 20 nm, electromagnetic energy is mainly distributed in the gap area between cylinder and the upper metal film.

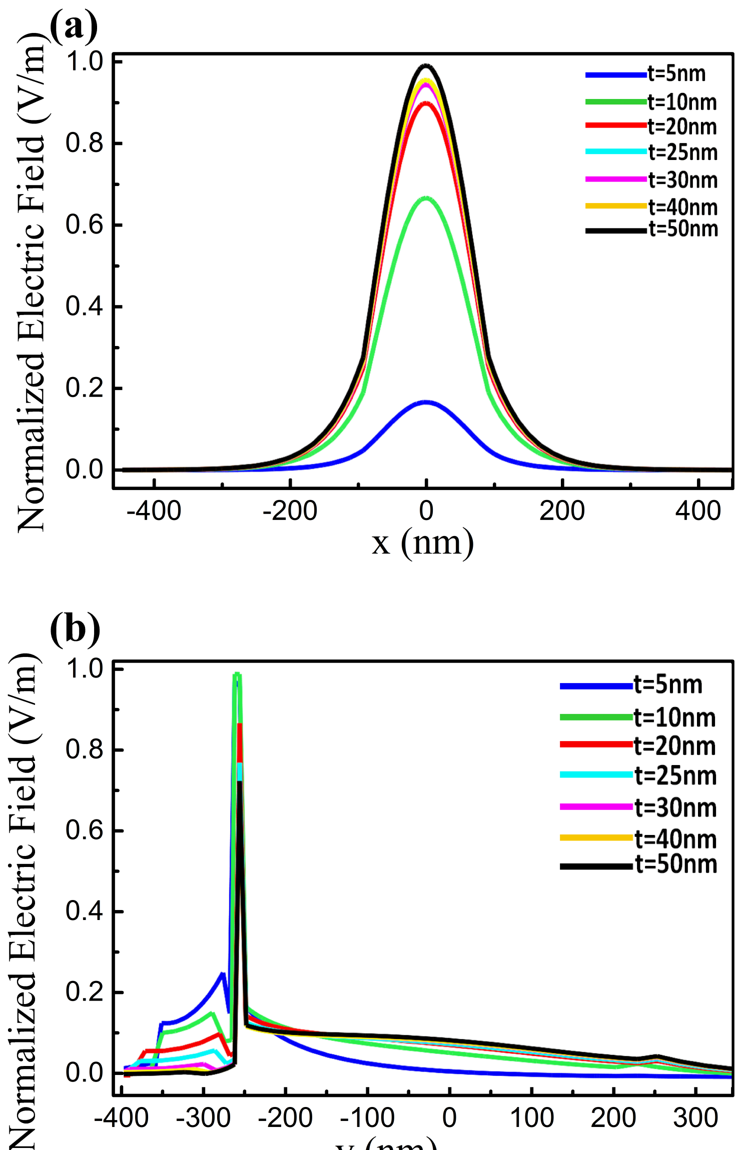


Figure S4: (a) Confinement of electric field E(x,y) distribution in the dielectric gap spacer region and the gap area between cylinder and the upper metal film with d = 500nm, h = 75 nm and g = 5nm along y = 0 with the variable metal film thickness t shown in the inset; (b) Confinement of electric field E(x,y) distribution in the dielectric gap spacer region and the gap area between cylinder and the upper metal film with d = 500nm, h = 75 nm and g = 5nm along x = 0 with the variable metal film thickness t.

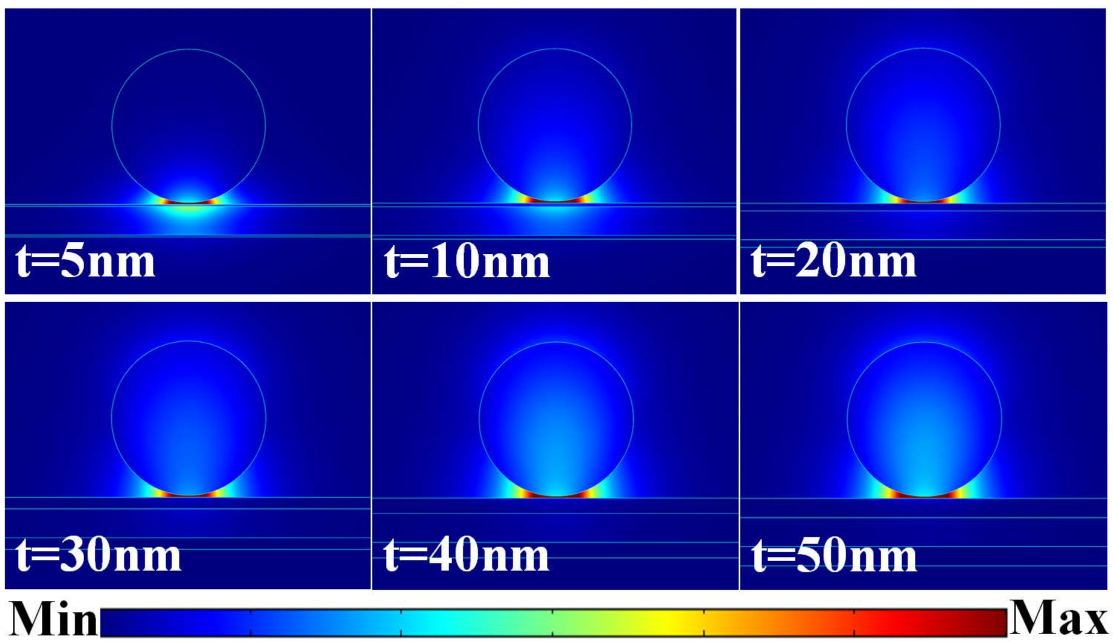


Figure S5: Electromagnetic energy density distributions with the variable metal film thickness t when d = 500 nm, g = 5 nm and h = 75 nm: When the metal film thickness is too small, such as 5 nm, part of the electromagnetic field energy would be distributed in the low dielectric layer; While, when t large enough, metal loss would be appeared, which offset the distribution of the electromagnetic field energy in low dielectric layer.

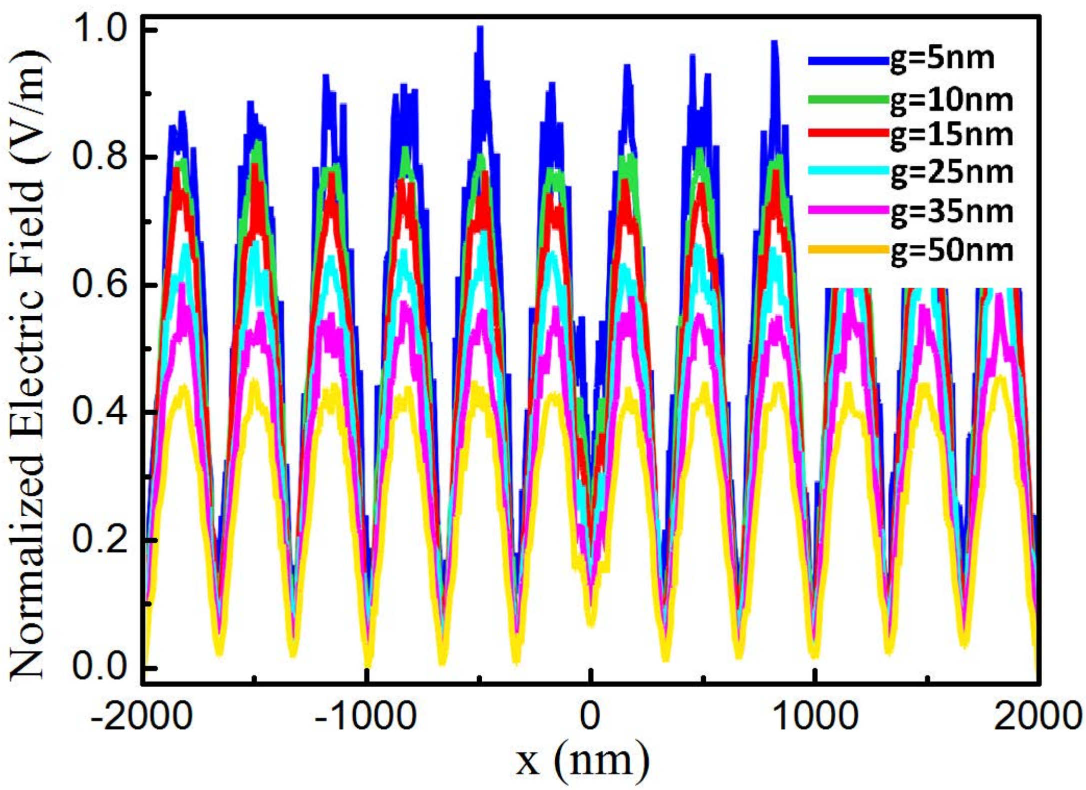


Figure S6: Electric field E(x,y) distribution in the dielectric gap spacer region with d = 500 nm, t = 10 nm and h = 20 nm along y = 0 with the variable gap g shown in the inset. It represents that when the spacer between two metal films is much small, electrical field would be confined in the spacer region.

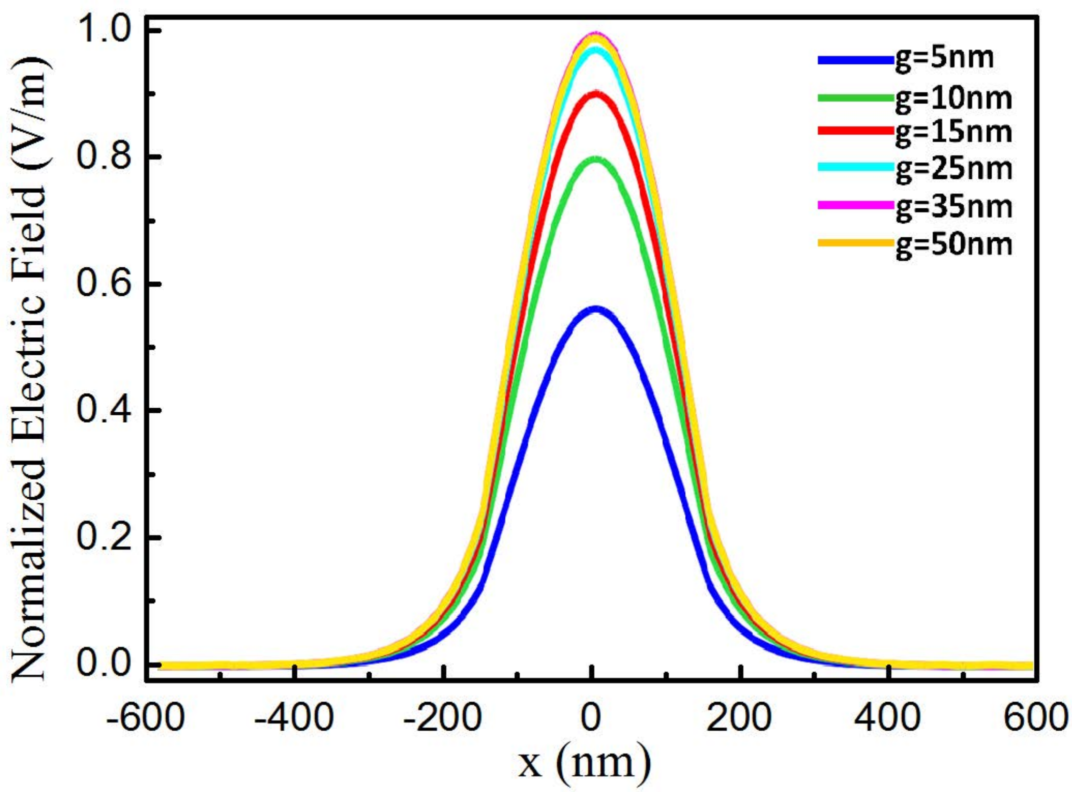


Figure S7: Electric field E(x,y) distribution in the dielectric gap spacer region with d = 500 nm, t = 10 nm and h = 75 nm along y = 0 with the variable gap g shown in the inset. It represents that obvious electrical field distribution would be transferred from the gap region between two metal films to the gap area between the cylinder and the upper metal film.

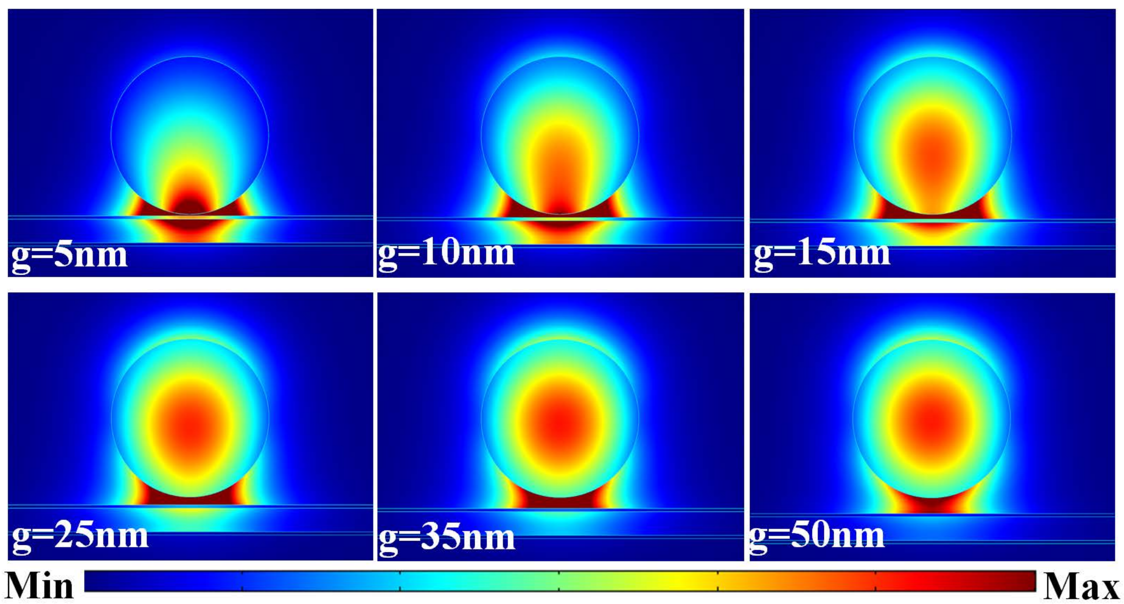


Figure S8: Electromagnetic energy density distributions with the variable gap distance between the cylinder and the upper metal film g when d = 500 nm, t = 10 nm and h = 75 nm: When the gap distance g is too small, such as 5 nm, part of the electromagnetic field energy would be distributed in the low dielectric layer; While, when g large enough, electromagnetic energy density distributed in the cylinder would be appeared, which offset the distribution of the electromagnetic field energy in low dielectric layer spacer.

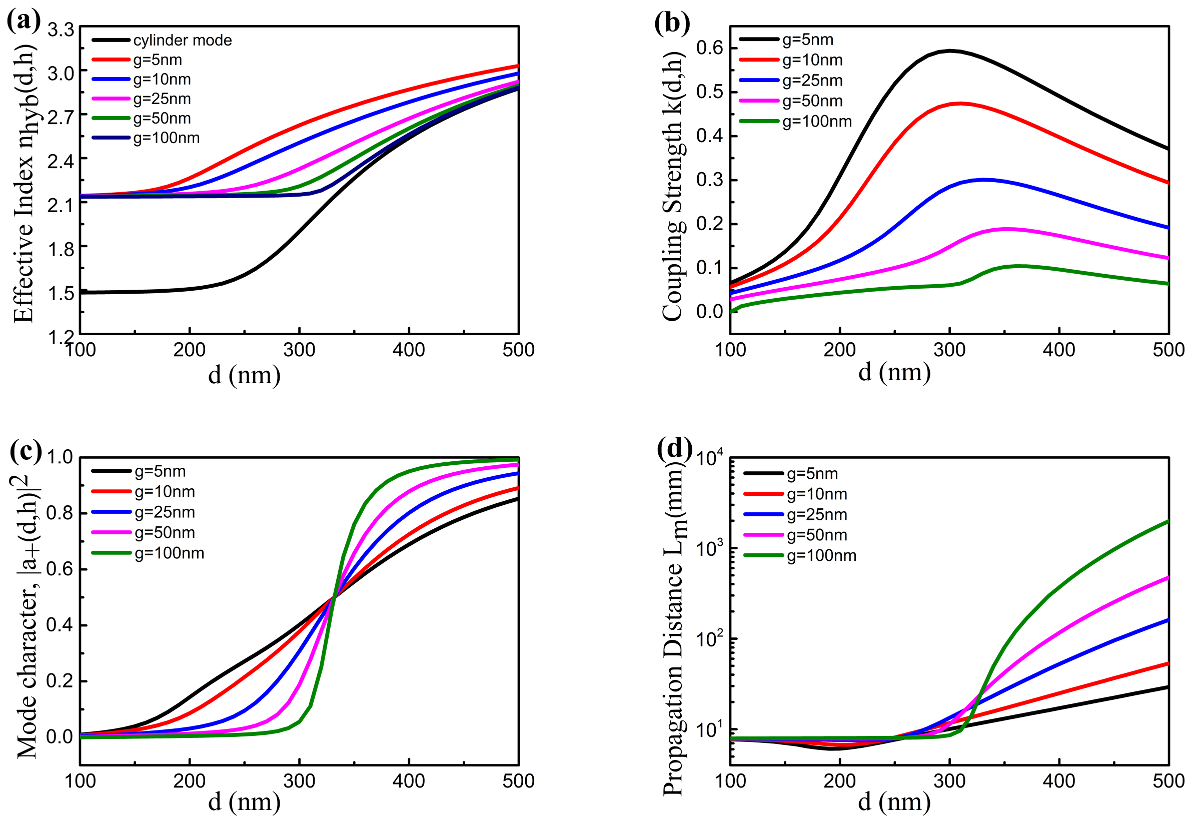


Figure S9: The mode characteristics of hybridized plasmonic waveguide for a range of gap widths g and cylinder diameters d when h=50 nm: (a) The mode effective index of the hybrid waveguide, the cylinder mode demonstrated shows significant difference from the hybrid plasmonic modes induced by double metal films; (b) Coupling strength $\kappa(d,h)$ dependent on the diameter of the cylinder and the dielectric spacer thickness; (c) When $|a_+(d,g)|^2 > 0.5$ the mode is cylinder-like and $|a_+(d,g)|^2 < 0.5$, the mode is SPPs-like modes, hence, $|a_+(d,g)|^2 = 0.5$ means that the maximum coupling occurs where the hybrid mode consists of equal proportions of cylinder and SPPs modes; (d) The hybrid modes propagation distance $L_m$.

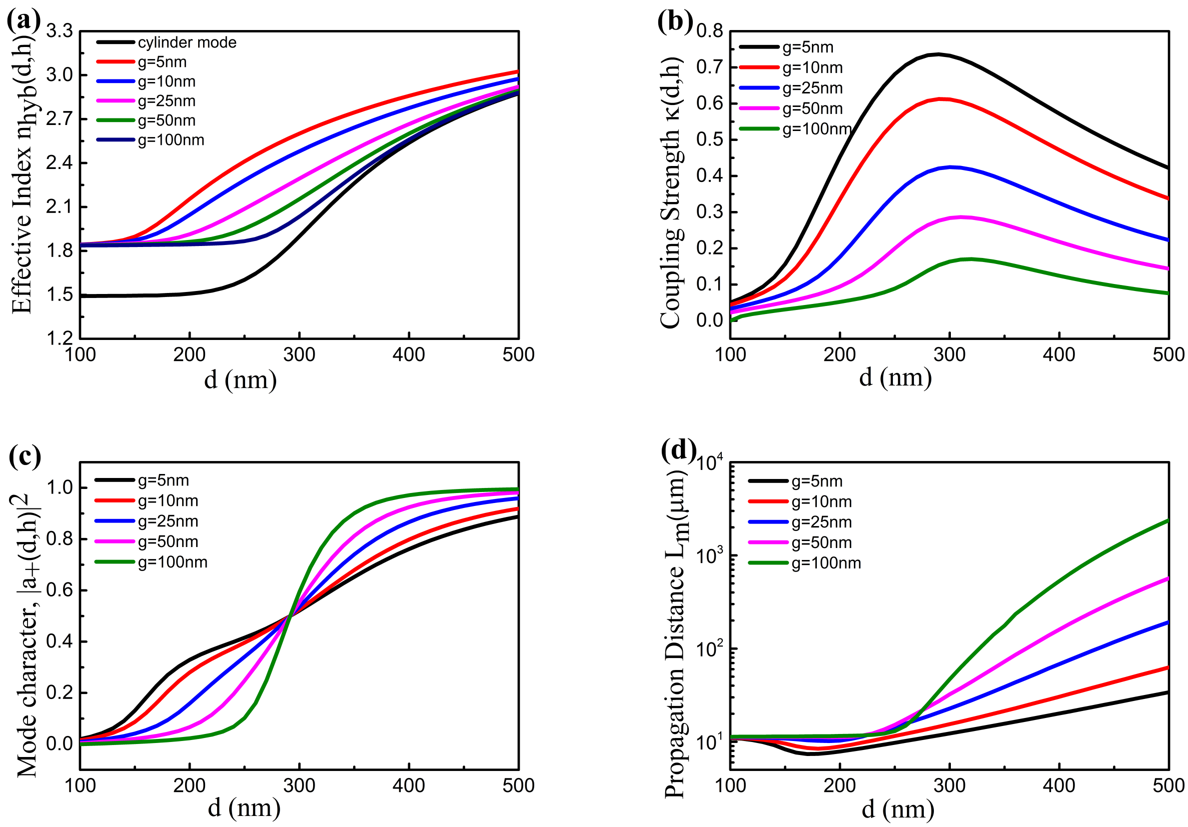


Figure S10: The mode characteristics of hybridized plasmonic waveguide for a range of gap widths g and cylinder diameters d when h=100 nm: (a) The mode effective index of the hybrid waveguide, the cylinder mode demonstrated shows significant difference from the hybrid plasmonic modes induced by double metal films; (b) Coupling strength $\kappa(d, h)$ dependent on the diameter of the cylinder and the dielectric spacer thickness; (c) When $|a_+(d, g)|^2 > 0.5$ the mode is cylinder-like and $|a_+(d, g)|^2 < 0.5$, the mode is SPPs-like modes, hence, $|a_+(d, g)|^2 = 0.5$ means that the maximum coupling occurs where the hybrid mode consists of equal proportions of cylinder and SPPs modes; (d) The hybrid modes propagation distance $L_m$.